CONF-8905113--1

SAND--89-0449C

DE89 008279

STUDIES OF OXIDATIVE DEGRADATION OF POLYMERS INDUCED BY IONIZING RADIATION

R. L. Clough and K. T. Gillen

Sandia National Laboratories, Albuquerque, New Mexico, 87185, USA

ABSTRACT

Radiation effects on polymers in the presence of air are characterized by complicated phenomena such as dose-rate effects and post-irradiation degradation. These time-dependent effects can be understood in terms of: 1) features of the free radical chain-reaction chemistry underlying the oxidation, and 2) oxygen diffusion effects. A profiling technique has been developed to study heterogeneous degradation resulting from oxygen diffusion, and kinetic schemes have been developed to allow long-term aging predictions from short-term high dose-rate experiments. Low molecular weight additives which act either as free-radical scavengers or else as energy-scavengers are effective as stabilizers in radiation-oxidation environments. Non-radical oxidation mechanisms, involving species such as ozone, can also be important in the radiation-oxidation of polymers.

KEYWORDS

Radiation effects, Oxidation, Polymer Degradation, Oxygen Diffusion, Stabilizers, Ozone, Dose-Rate Effects.

INTRODUCTION

The effects of ionizing radiation (i.e., gamma, x-ray, electron beam, etc.) are of growing interest because of increasing applications involving the radiation-processing of polymers, and also because of the use of polymeric materials in applications involving long-term radiation environments. Many of the important applications involve air-atmosphere environments. The primary events in the interaction of high-energy radiation with organic polymeric materials involve: 1) ionization followed by electron-cation recombination to yield highly excited electronic states of the molecules, followed by 2) dissociation of a portion of the excited states to yield reactive species, most importantly free radicals. During the 1950's and 1960's, polymer radiation effects were most extensively studied in the absence of the "complicating effect" of oxygen. A number of results came out of these studies which became widely known (1-4), including: 1) well-defined tables of structure/property relationships cataloging various polymers as to whether they undergo primarily crosslinking or scission upon exposure to ionizing radiation, 2) tables showing relative radiation-dose tolerances of different polymers to ionizing radiation, and 3) evidence that equal dose gives rise to equal damage, regardless of the dose rate.

In the presence of oxygen, polymer radiation effects often differ significantly compared with inert-atmosphere irradiation, and can exhibit very complicated phenomena. Radiation damage at an equivalent dose may be far more extensive when oxygen is present. The scission/crosslinking classifications no longer apply; scission is often more highly favored under oxidative conditions. Furthermore, both the extent and the nature of the radiation-induced material changes often exhibit strongly time-dependent behaviors, including dose-rate effects and post-irradiation effects. These behaviors make it extremely difficult in air-containing environments to anticipate the nature of long-term radiation-induced changes in materials, or to predict useful material lifetimes. Our work has been aimed at obtaining detailed understanding of mechanisms underlying radiation-induced effects on polymers in oxidizing environments, and applying this information to solving materials degradation problems (5-10).

RESULTS AND DISCUSSION

Figures 1, 2 and 3 are examples of radiation-induced mechanical property changes in polymeric materials obtained in our laboratories, illustrating: 1) inert atmosphere versus air atmosphere irradiation (11), 2) dose rate effects (5) and 3) post-irradiation degradation (5). Many other dramatic examples of time-dependent effects in air irradiations have been reported by other workers. For instance, Horng and Klemchuk (12) determined the breaking angle in polypropylene samples to be 70^{o} immediately after irradiation to a dose of 2.5 Mrad (compared with a value of 90^{o} in unirradiated material). After standing at room temperature in an air atmosphere for 6 months subsequent to irradiation, the breaking angle of the material had decreased to less than 20^{o}. As another example, Wilski (13) reported on the rupture time of highly-pressurized polyethylene pipes. Pipes which had been irradiated to a dose above 20 Mrad at a dose rate of 100 Mrad/h had their rupture times increased by 100 fold, whereas pipes irradiated to a dose of 5 Mrad at a dose rate of 400 rad/h had their rupture times decreased by a factor of 10^{4}.

Time-dependent effects can be understood in terms of two mechanisms which affect the radiation-induced oxidation: "physical" effects (caused by oxygen diffusion as a rate-limiting step in the oxidation chemistry) and "chemical" effects (which occur whenever a reaction step in the chemical oxidation pathway has a time-scale which is on the same order as the experimental time-frame).

Profiling Heterogeneous Oxidation

Oxygen diffusion effects arise very frequently for polymeric materials irradiated in the presence of air. This effect is controlled by the oxygen permeation coefficient of the polymer, the dose rate, the inherent radiation-oxidation yield of the polymer, and the material thickness.

Oxygen diffusion can become rate limiting whenever dissolved oxygen in the material is consumed by reaction with free radicals (generated by the radiation) faster than oxygen can be replenished from the surrounding atmosphere by diffusion through the material. When diffusion effects are important, the result is heterogeneous degradation such that extensive oxidation occurs in the regions near the sample surfaces, whereas a lower degree of oxidation (or no oxidation) occurs in the sample interior. In high dose rate experiments, oxidation only in regions near the sample surfaces is a frequent occurrence (6,8). Irradiation of samples at a lower dose rate results in oxidation deeper into the sample interior; at a sufficiently low dose rate, homogeneous oxidation throughout the sample will occur. Because of the large differences in radiation effects involving oxidizing versus non-oxidizing conditions (as discussed above), the extent of oxidative penetration often has a very large effect on radiation-induced material changes. This gives rise to the observation of a dose-rate effect, most typically involving a degree of molecular change (damage) per equivalent absorbed dose which is larger at lower dose rate.

A number of means have been developed to identify the occurrence of heterogeneous degradation (14). Most of the techniques involve slicing the sample into many small pieces (from edge to center), and performing a separate analysis on each piece using infrared analysis, chemiluminescence, gel permeation chromatography, or other technique. We have developed a convenient technique for rapid and quantitative profiling of heterogeneous oxidative degradation on intact samples, which we call modulus profiling (8,6). By this technique, a sample is cut in cross-section and held in a tiny vise. The depth of indentation into the material of a tiny, weighted probe is determined as a function of position on the cross-sectional surface. A schematic diagram of this instrument (8) is provided in figure 4. By this method, we are readily able to obtain detailed profiles of heterogeneous degradation for samples as thin as 1 mm or less. Figures 5 and 6 illustrate heterogeneous profiles obtained by modulus profiling of ethylene-propylene rubber (EPR) materials as a function of material thickness and dose rate.

"Chemical" Time-Temperature Effects

The second type of effect underlying time-dependent degradation behaviors, which may be referred to as a chemical effect, involves the time/temperature-dependent rate of oxidative chemical reaction of a reactive organic species. The species most often responsible for this phenomenon are trapped radicals or peroxides. A set of equations for the principal radical reactions underlying radiation-oxidative degradation is presented in Figure 7. Post-irradiation oxidation occurs when radicals formed by the irradiation, which are of low reactivity, continue to react with oxygen during subsequent storage of the samples in air. For example, if the radicals are formed in a crystalline region of the material, they will slowly migrate out to amorphous regions and come into contact with oxygen, at which time the radical propagation steps can then proceed. In addition, peroxides formed during the course of the irradiation can undergo thermal decomposition, providing a chain branching step which yields free radicals

that can then participate (5) in oxidation-propagation steps. Dose-rate effects can similarly arise from slow reaction of peroxides or radicals. These time-dependent chemical processes may make small or negligible contributions for the time-scales of high-dose rate experiments (which may last days), but can make extremely large contributions to the oxidation occurring for low dose rate exposures (which may last months or years).

Predictive Aging Experiments

The ability to make reliable predictions of long-term aging rates of materials is essential for assessing the relative performance of materials or formulations being developed for optimized radiation resistance. It is also a requisite for stipulating a material lifetime for a particular application environment of interest. Keeping in mind the mechanisms underlying time-dependent effects in radiation-oxidative degradation, it is possible to devise meaningful experimental techniques for long-term aging predictions. Two separate situations will be discussed in turn: 1) predictions for materials placed in use or in storage for long time periods following an initial short-term radiation exposure, and 2) predictions for materials used in applications having long-term radiation exposure. The first of these two situations requires the ability to make predictions for materials having post-irradiation effects. The second situation, which is the more difficult and is the area in which we have expended the most effort, requires the ability to make predictions for materials having strong dose-rate effects.

A useful approach for predicting post-irradiation degradation rates is entirely analogous to the standard Arrhenius methodology which is widely used for accelerated thermal aging experiments for polymers. The Arrhenius approach assumes that the time-dependency of a thermal aging process can be understood in terms of an "apparent" activation energy underlying the relevant rate-limiting steps. Aging experiments are performed at a series of different temperatures chosen to be higher than ambient, and the change in some property of interest is followed as a function of time. A plot is made of the log of the time required to reach an arbitrary amount of damage, versus the reciprocal temperature (in ^{o}K). For experimental aging plots which yield straight-line (i.e., "Arrhenius") behavior, an extrapolation may be attempted to a selected temperature corresponding to a longer-time-period experiment. In the case of post-irradiation degradation, the same experimental treatment can be carried out, except that the thermal aging is performed on samples which have been pre-irradiated using the same irradiation parameters (including dose, dose rate and radiation type) as will be used in the actual application. When post-irradiation effects significantly larger than thermal degradation rates for unirradiated samples are found, these can be associated with oxidation chemistry involving reactive species previously formed by irradiation, such as long-lived radicals or peroxides. Figure 8 provides an example of an Arrhenius aging plot (based on the data in Figure 3) for a PVC material which was pre-irradiated to a dose of 6 Mrad at 4.4 krad/h and 25^{o}C. In this case, the

immediate effect of the irradiation was to lower the tensile elongation to 86% of the initial value. The data given in the figure show the time required to lower the elongation to 60% of the initial value at three post-irradiation temperatures: 70°C, 78°C and 90°C. (Note by way of comparison that treatment of unirradiated material at 90°C for the same experimental time period gave rise to no measurable change in tensile elongation). Extrapolation yields a prediction that a time of about 9 years would be required to reduce the elongation of the preirradiated samples to 60% of initial in the case of material held at room temperature (25°C). From the slope of the line, an apparent activation energy for the aging process of 21 kcal/mol is obtained. Note that in this example, only three experimental aging temperatures were used, which is a minimal amount of data for such an extrapolation. As with the standard Arrhenius approach for thermal aging, confidence in predictions is enhanced by using data from as many different temperatures as is reasonably possible for the extrapolation. Furthermore, the lowest-temperature aging simulation should be as near to the desired ambient environmental temperature as is possible given the experimental time frame available. Other Arrhenius-method considerations also apply. For instance, extrapolations through a physical transition temperature of the material (e.g., T_g or T_m) must be avoided. Experiments at sufficiently high temperatures as to result in rate-limiting processes (such as oxygen diffusion effects), which are different from those important at the application temperature, must be avoided.

Predictions involving long-term, low-level radiation environments, where significant dose-rate effects can arise, may be dealt with by an approach which considers the underlying mechanisms of these effects (7,9). We start by analyzing the raw data to generate a plot showing the dose required to cause an equivalent amount of damage, as a function of experimental dose rate and temperature conditions. This is illustrated for a chlorosulfonated polyethylene (Hypalon) material in Fig. 9, where the damage criterion chosen is the dose required to reduce the tensile elongation to 50% of initial, for each set of experimental conditions. Data corresponding to samples which were heterogeneously oxidized (triangles) must first be eliminated from consideration, since no meaningful extrapolation based on heterogeneous data is generally possible. These data can be identified by direct profiling of the samples, or by calculation (9) using the oxygen permeation constant and radiation-oxidation yield for the material (if the latter data are available). For the remaining homogeneous data (circles), we then assume that an Arrhenius activation energy will be applicable for the time/temperature dependence of that part of the dose rate effect which arises due to slow oxidation chemistry involving reactive species produced by the irradiation (peroxides or radicals). This allows us to horizontally shift the homogeneous data to a selected reference temperature using various trial activation energies, looking for an empirical activation energy that results in reasonable superposition of the shifted data. The homogeneous data of Fig. 9, for example, were found to give excellent superposition, as shown in Fig. 10, when horizontally shifted

using a 24 kcal/mol activation energy. Such superposed results allow predictions to be made at very low (experimentally inaccessible) dose rates. Further details of the shifting procedure, and its mechanistic basis, are outside the scope of this paper, and are presented in references 7 and 9.

Stabilizers For Radiation-Oxidation Degradation Environments

There are extensive ongoing efforts directed toward identifying effective stabilizer additives for use in environments of ionizing radiation. Most of the work has centered on the use of antioxidant molecules which are known to be effective stabilizers against thermo-oxidative degradation, and which operate by scavenging radicals. A number of such radical scavengers have been found to offer significant protection, both in cases of post-irradiation oxidation and in cases of long-term, low-level irradiation. In a number of the studies involving the latter environment, however, oxygen diffusion effects were not considered with respect to the high-dose-rate experiments employed, so that it is not clear whether the data obtained pertain to primarily oxidizing or non-oxidizing conditions. An excellent example of post-irradiation oxidation stabilization was provided by Carlsson, Wiles and co-workers (15), who found that polypropylene films irradiated to 2 Mrad and subsequently held at 60°C in air underwent extensive oxidation (as seen by IR spectroscopy) over the course of two days, during which time the elongation at break decreased to essentially 0%. However, in similarly-irradiated samples containing any of three different types of antioxidant additives, only minimal post-irradiation oxidation, accompanied by a reduction in elongation to no more than 50% of initial, occurred after one month at 60° in air.

Figures 11 and 12 provide a detailed example from our own laboratories (16) on the effect of certain additives on a polychloroprene material which was continuously irradiated under low-dose-rate conditions in the presence of air (20 krad/h at 45°C). By means of our modulus profiling apparatus, we were able to establish that homogeneous oxidation occurred under these conditions. The study included samples of the polychloroprene prepared with no additive and with 1.7 % by weight of the hindered phenol antioxidant 2,2-methylene bis(4-methyl-6-t-butylphenol). Another type of additive, which has been previously studied with respect to enhancing radiation resistance under inert-atmosphere conditions, is comprised of molecules which are effective scavengers of excited state energy. We expected that such molecules should also exert a significant effect under radiation-oxidation conditions, by deactivating some of the initially-formed excited states back to the ground state and thereby reducing the total number of radicals subsequently formed in the system. We therefore prepared polychloroprene samples containing 1.7 % by weight of a molecule which we expected to function in this way (a polycyclic aromatic hydrocarbon: pyrene). As indicated in Figure 11, the rate of deterioration in tensile elongation is significantly reduced in materials containing either the radical scavenger or the energy scavenger. Also, the energy-scavenger additive is seen to

result in significant improvement not only when used alone but also in the presence of a radical scavenger. Figure 12 presents data on the reactive loss of the radical scavenger additive, and provides insight on the dose at which this molecule is consumed by radiation-induced radical chemistry. These data were obtained by exhaustive solvent extraction of degraded samples followed by gas chromatographic analysis. The percent of recovered phenolic antioxidant is seen to be reduced by an order of magnitude following 20 Mrad exposure under oxidizing conditions. Note that this data provides evidence that an energy scavenger additive in low concentration functions not only to protect the polymer directly, but also acts to protect the antioxidant stabilizer. For example, the amount of hindered phenol remaining following 20 Mrad is approximately two times higher in samples containing pyrene. If the pyrene performs its stabilizing function by the mechanism discussed above (trapping excited-state energy, followed by decay to the ground state), this should be a non-destructive process for the pyrene molecule. This is in contrast to the radical scavenging mechanism, for which the scavenger molecule undergoes chemical reaction in the course of trapping a radical. Extraction data for the pyrene (also shown in Fig. 12) indicate that it indeed survives in the polymer to much higher doses compared with the antioxidant. For example, at 30 Mrad, more than 90% of the initial pyrene concentration is still present both in the presence and absence of the antioxidant.

Non-Radical Radiation Oxidation Mechanisms

As discussed above, the most important and extensively studied mechanism of radiation-induced oxidation chemistry is that mediated by free radicals formed within the polymer matrix under the influence of the radiation exposure. However, we have recently obtained evidence of a non-radical chemical mechanism playing an important role in the radiation-degradation of certain materials (17). Relevant data are summarized in Figure 13, which presents modulus profiles for styrene-butadiene copolymer samples subjected to gamma radiation (84 Mrad at 0.5 Mrad/h, at 25°C). The solid circles indicate the flat profile of an unaged sample. The solid squares show an interesting "W" shaped profile for a sample irradiated in the presence of air. We were readily able to assign the broad, internal profile to the usual oxygen diffusion effects pertaining to the standard free radical oxidation mechanism. Note that the diamond-shaped symbols pertain to a sample irradiated under vacuum. As could be expected, the modulus value of the flat profile obtained in the absence of oxygen corresponds closely to the modulus value at the interior (oxygen-starved) region of the air-irradiated sample. We hypothesized that the strong degradation effect seen in the surface regions of the sample arose due to attack by reactive gaseous species generated by the action of the radiation on the air atmosphere surrounding the sample. Ionizing radiation can indeed produce virtually every imaginable molecular species from the atoms available in a given mixture (whether gaseous, liquid or solid). For example, products identified as arising from the radiolysis of air include NO, NO_2, O_3, N_2O_5, and others (18). The question to be addressed is whether any such species

can be competitive with the highly-effective radical oxidation mechanism in causing radiation oxidation of polymers.

We have been able to show (17) that the strong degradation effect in the surface regions of the styrene-butadiene material was due to the radiolysis product, ozone. Two key pieces of experimental evidence are summarized below. First, irradiation of a sample of the material under an atmosphere containing 20% O_2 and 80% argon resulted in a profile nearly the same as that produced upon air irradiation. This indicates that if the surface-region effect indeed results from attack by a gaseous species, that species is derived from oxygen alone. Secondly, we impregnated glass wool with a specific chemical trap for ozone (potassium iodide), and wrapped a cocoon of this material around a sample of the styrene-butadiene material prior to irradiation. Our expectation was that if the surface-region degradation were indeed due to attack by ozone, the impregnated glass wool should act as a selective filter which would eliminate the surface region degradation, while leaving the broad interior profile (due to oxygen diffusion) unchanged. This was exactly the result obtained, as indicated by the profile represented by the open squares in Figure 13. We also found that the modulus profile obtained after irradiating a sample surrounded by a cocoon of unimpregnated glass wool exhibited the strong edge-region effect found with samples irradiated without any cocoon, indicating that the glass wool impregnated with potassium iodide really acted as a specific chemical trap rather than just providing a high-surface-area filter.

Note that ozone-mediated degradation (which has been extensively studied in urban atmospheres and other environments not involving ionizing radiation) is usually associated with samples under mechanical stress; however, the strong degradation effect which we have identified in these studies occurred in the absence of any applied mechanical stress. Based on experiments using ozone from a laboratory ozone generator, we obtained evidence that the ozone and simultaneously-applied radiation can be strongly synergistic in their effect on the polymeric material (17). We have also obtained evidence that the ozone mechanism may be generally important in polymers having double bonds along the chain, as is the case with the styrene-butadiene material discussed above. For example, we have found a strong "W" shaped degradation curve for Buna-N rubber (a copolymer based on acrylonitrile and butadiene). This conclusion is consistent with the high reactivity known for ozone towards double bonds.

REFERENCES

1. A. Charlesby, Atomic Radiation and Polymers, Pergamon Press, N. Y., 1960.

2. A. Chapiro, Radiation Chemistry of Polymeric Systems, Wiley, New York, 1962.

3. R. O. Bolt and J. G. Carroll, Radiation Effects on Organic Materials, Academic Press, 1963.

4. H. Schonbacher and A. Stolarz-Izycka, Compilation of Radiation Damage Test Data, Part I: CERN 79-04, Part II CERN 79-08, European Organization for Nuclear Research, Geneva, 1979.

5. R. L. Clough and K. T. Gillen, J. Polym. Sci., Polym. Chem. Ed., 19, 2041 (1981).

6. R. L. Clough, K. T. Gillen and C. A. Quintana, J. Polym. Sci., Polym. Chem. Ed., 23, 359 (1985).

7. K. T. Gillen and R. L. Clough, J. Polym. Sci., Polym. Chem. Ed., 23, 2683 (1985).

8. a) K. T. Gillen, R. L. Clough and C. A. Quintana, Polym. Deg. Stab., 17, 31 (1987); b) K. T. Gillen and R. L. Clough, Polym. Eng. and Sci., 29, 29 (1989).

9. K. T. Gillen and R. L. Clough, Polym. Deg. Stab., 24, (1989) in press.

10. R. L. Clough, Radiation Resistant Polymers, in: Encyclopedia of Polymer Science and Engineering, Volume 13, Second Edition, Wiley, New York, 1988, p. 667.

11. R. L. Clough and K. T. Gillen, to be published.

12. P. L. Horng and P. P. Klemchuk, Plast. Eng., April, 35 (1984).

13. H. Wilski, Kunststoffe, 58, 18 (1968).

14. K. T. Gillen and R. L. Clough, Techniques for Monitoring Heterogeneous Oxidation of Polymers, in: Handbook of Polymer Science and Technology, Volume 2, Marcel-Dekker, New York, 1989, p. 167.

15. D. J. Carlsson, C. J. B. Dobbin, J. P. T. Jensen and D. M. Wiles, in: P. Klemchuk (ed.), Polymer Stabilization and Degradation, ACS Symposium Series 280, American Chemical Society, Washington D. C. (1985), p. 373.

16. R. L. Clough and K. T. Gillen, to be published.

17. R. L. Clough and K. T. Gillen, J. Polym. Sci.: Part A, Polym. Chem. (1989) in press.

18. A. R. Anderson, Inorganic Gasses, in: P. Ausloos (ed.), Fundamental Processes in Radiation Chemistry, Wiley, New York, 1968, p. 311.

ACKNOWLEDGEMENTS

The authors are grateful to M. Malone and N. Dhooge, who performed most of the experimental work. This work was supported by the U. S. Dept. of Energy under contract number DE-AC04-76DP00789.

Fig. 1. Relative elongation of γ-irradiated samples (0.28 mm-thick) of poly(ethylene-co-tetrafluoroethylene) [Tefzel], comparing samples irradiated at 70°C with and without the presence of oxygen. □ = irradiation in air at 0.58 Mrad/h, ○ = irradiation under vacuum at 0.77 Mrad/h.

Fig. 2. Relative elongation of a PVC material irradiated at 60°C in air at a series of different dose rates. × = 0.94 Mrad/h, + = 0.36 Mrad/h, △ = 0.071 Mrad/h, ○ = 0.018 Mrad/h, □ = 0.0035 Mrad/h.

Fig. 3. Relative elongation of a PVC material showing post-irradiation degradation of samples held at three different temperatures. ○ = 90°C, △ = 78°C, □ = 70°C. The samples had been pre-irradiated to a dose of 6 Mrad at 4.4 krad/h in air at 25°C, which resulted in an immediate lowering of the elongation to 86% of the initial value.

Fig. 4. Schematic diagram of modulus profiling apparatus. A mass, M, is weighted into the sample. The indentation distance of the probe is measured using a linearly variable differential transducer (LVDT) from a Perkin-Elmer thermomechanical analyzer. Three identical polymer samples (S) are held in a sandwitch arrangement, and a profile is obtained across the exposed (cross-sectional) surface of the central sample. The samples are held together between opposing metal plates (P).

Fig. 5. Edge-to-edge modulus profiles of ethylene-propylene rubber of three different thicknesses following γ-irradiation at 0.67 Mrad/h at 70° in air for the time-periods indicated. The dashed line represents the flat profile of unaged material. P denotes the percentage of the distance from one air-exposed surface to the opposite air-exposed surface. Sample thicknesses were: A = 2.7 mm, B = 1.7 mm, C = 0.7 mm.

Fig. 6. Edge-to-edge modulus profiles of ethylene-propylene rubber samples 1.7 mm thick, following γ-irradiation at 70°C in air at two different dose rates. P denotes the percentage of the distance from one air-exposed surface to the opposite air-exposed surface. △ - unirradiated material, ○ - 0.11 Mrad/h to a dose of 174 Mrad, □ - 0.67 Mrad/h to a dose of 225 Mrad.

Fig. 7. Outline of the primary free radical reactions underlying the radiation-induced oxidation of polymers.

Fig. 8. Arrhenius plot based on data of Figure 3, showing the post-irradiation time required to reduce the elongation of PVC materials to 60% of initial, as a function of reciprocal temperature (in °K). Extrapolation to a temperature of 25°C (arrow) yields a prediction that approximately 9 years is required to reduce the elongation to 60% of initial at this temperature.

Fig. 9. Dose to equivalent damage (DED) plot, showing radiation dose required to reduce the elongation of a chlorosulfonated polyethylene (Hypalon) material to 50% of its initial value. The data were taken from radiation experiments run under a variety of different dose rates and temperatures. (The numbers beside the data points represent the experimental temperature in °C). The dashed curve represents the approximate dividing line found between heterogeneously-oxidized and homogeneously-oxidized samples.

Fig. 10. Dose to equivalent damage (DED) data from Figure 10 after time-temperature-dose-rate shifting to a reference temperature chosen to be 45°C. The curve predicts the time required at this temperature to reduce the tensile elongation of this material to 50% of the initial value as a function of dose rate.

Fig. 11. Relative tensile elongation for polychloroprene material as a function of dose. Samples were γ-irradiated at 0.02 Mrad/h at 45°C in air. ◇ - material containing no stabilizer additive, ○ - material containing 1.7 % of the antioxidant 2,2-methylenebis(4-methyl-6-t-butylphenol), △ - material containing 1.7% pyrene, □ - material containing 1.7% each of pyrene and 2,2-methylenebis(4-methyl-6-t-butylphenol).

Fig. 12. Weight fraction of additive recovered from irradiated polychloroprene samples described in Figure 12. □ - 2,2-methylenebis(4-methyl-6-t-butylphenol) recovered from samples not containing pyrene, ○ - 2,2-methylenebis(4-methyl-6-t-butylphenol) recovered from samples which also contained pyrene, △ - pyrene recovered from samples, either in the presence or absence of the antioxidant.

Fig. 13. Edge-to-edge modulus profile through the cross-section of 1.9-mm thick poly(butadiene-co-styrene) following γ-irradiation at 0.5 Mrad/h to a dose of 84 Mrad at ambient temperature (25°C). ● - unirradiated material, ■ - irradiated in air, □ - irradiated in air, while surrounded with a 0.5-mm thick glass wool cocoon impregnated with KI, ⊕ - irradiated under vacuum.

Relative Elongation of Irradiated Tefzel

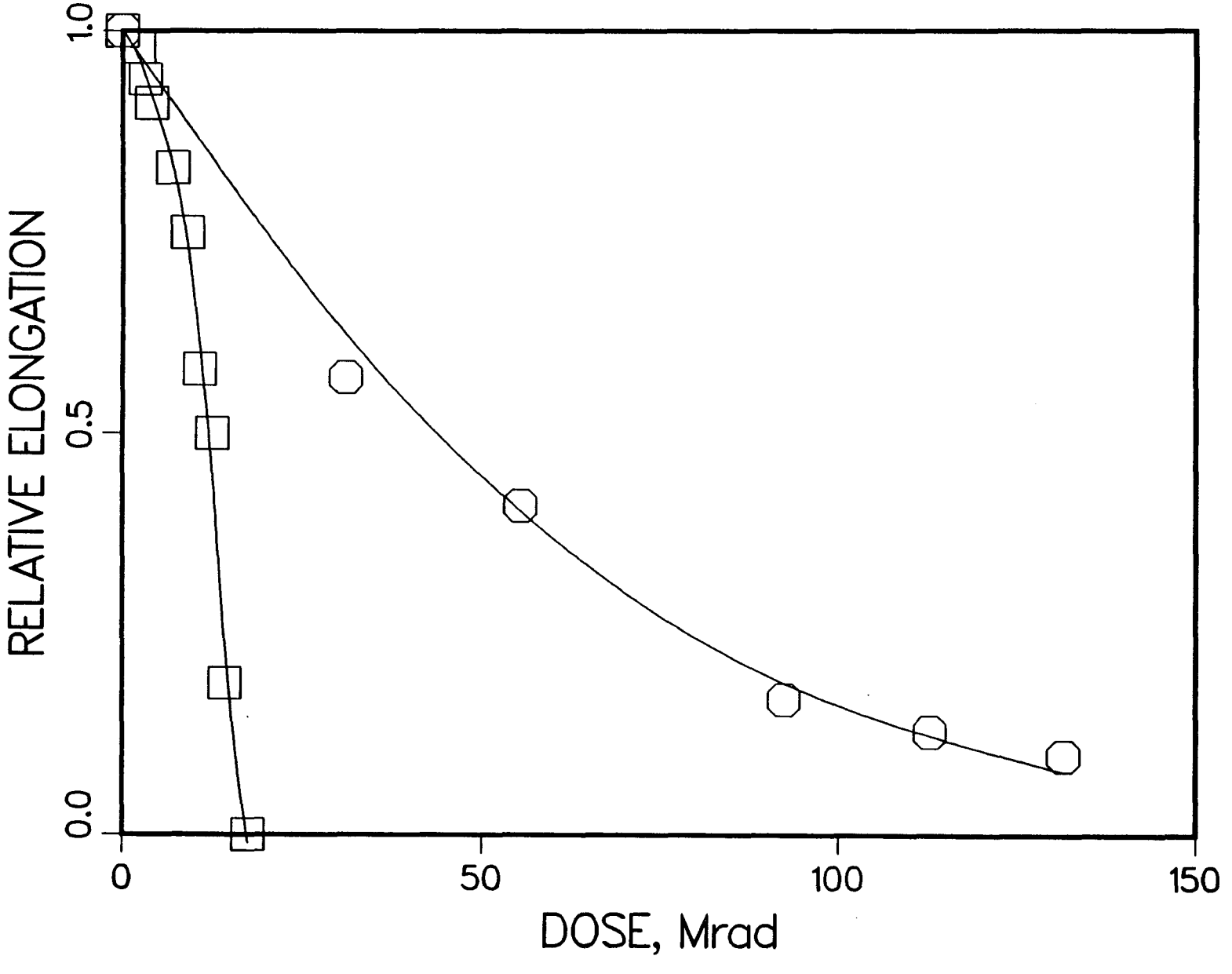

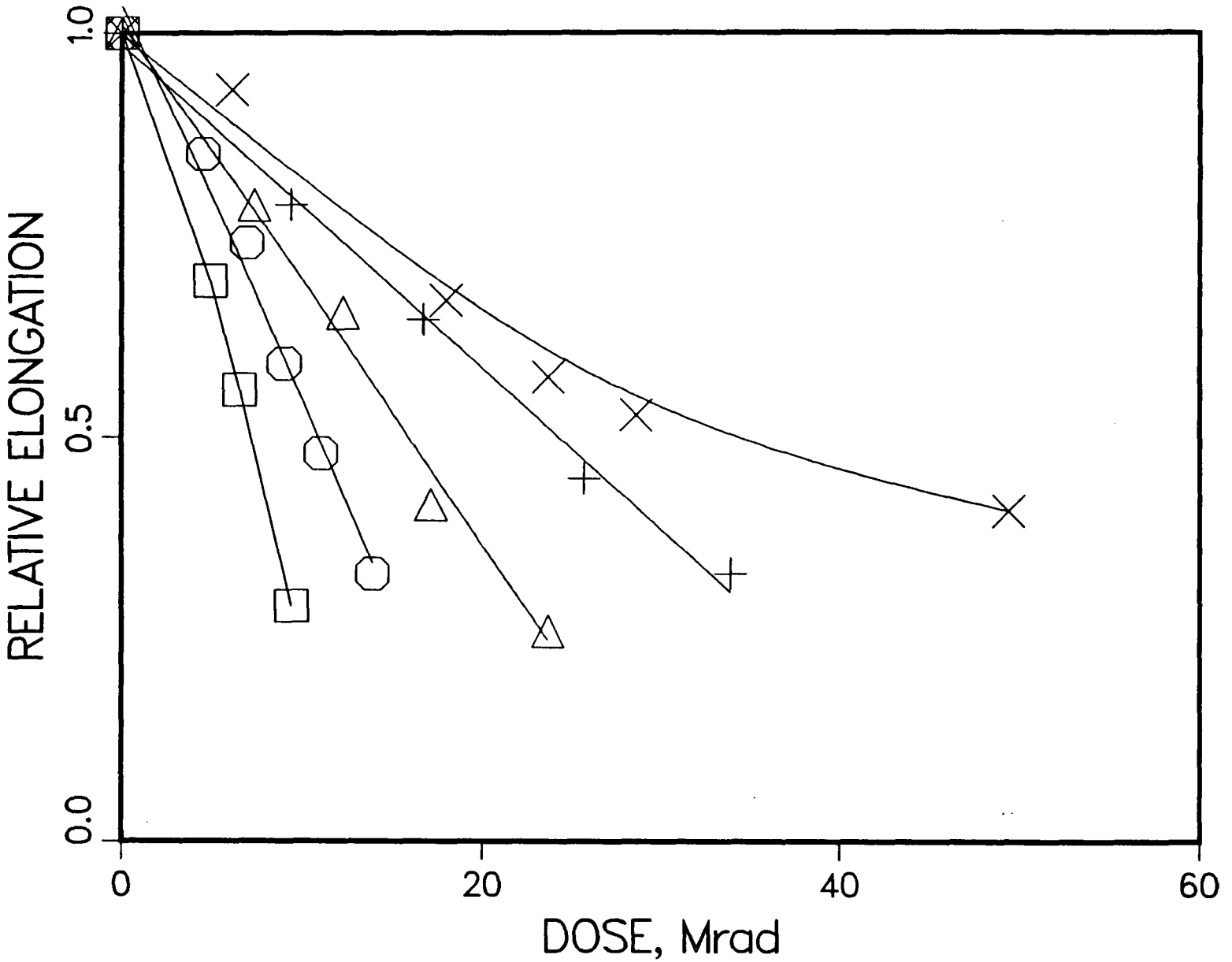
RELATIVE ELONGATION
1.0
0.5
0.0
0
20
40
60
DOSE, Mrad

Relative Elongation of Irradiated PVC

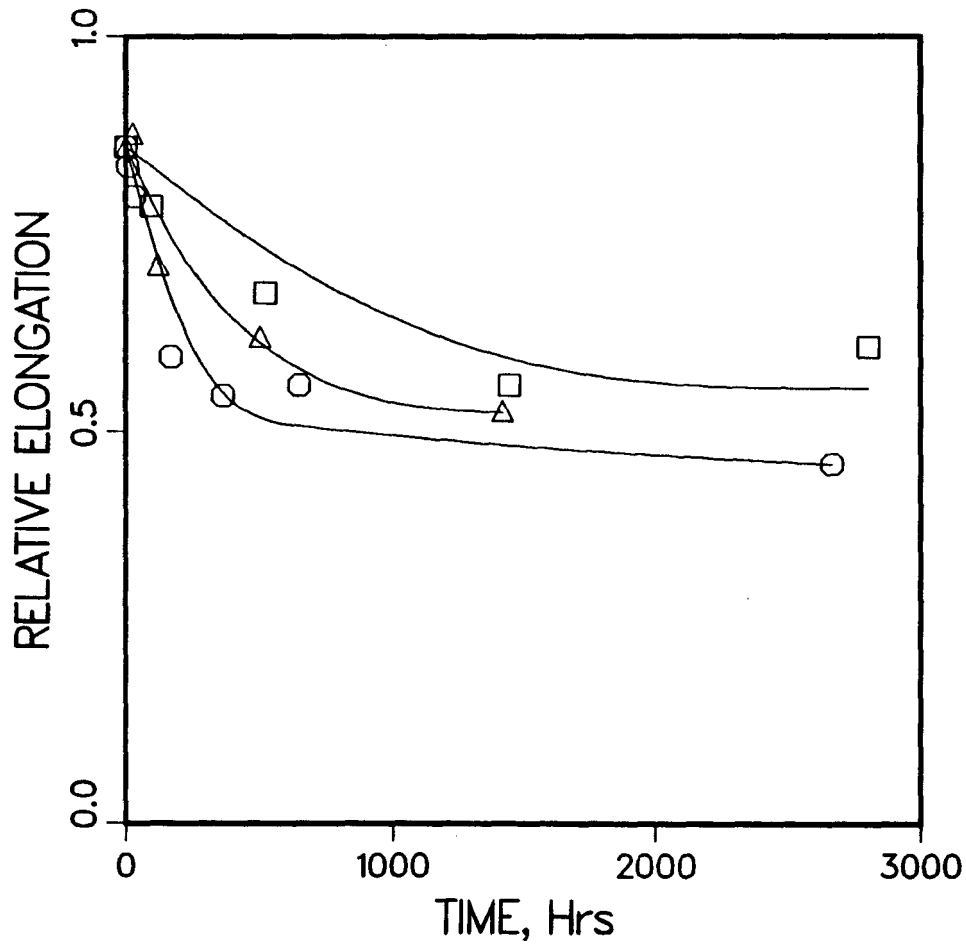

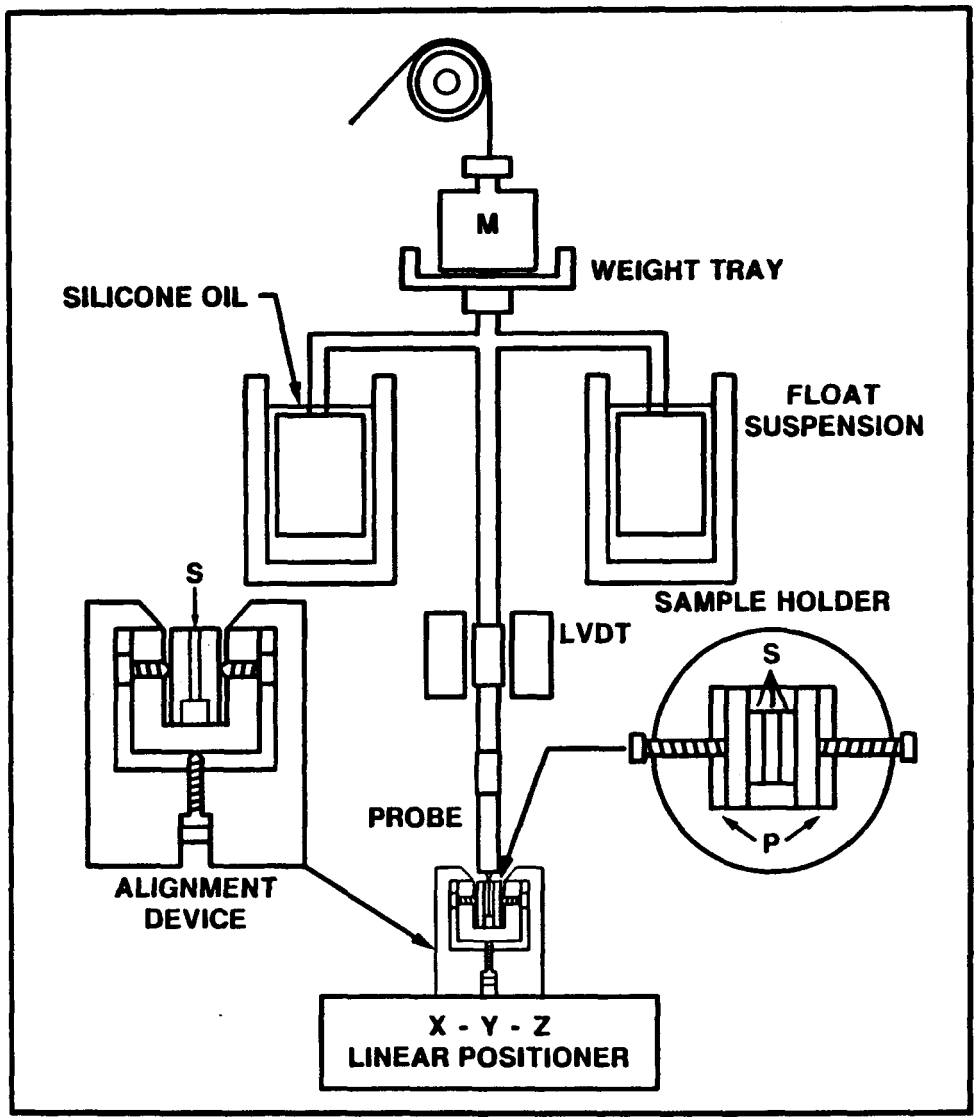

SCHEMATIC DIAGRAM OF MODULUS PROFILING APPARATUS

88W1000.50

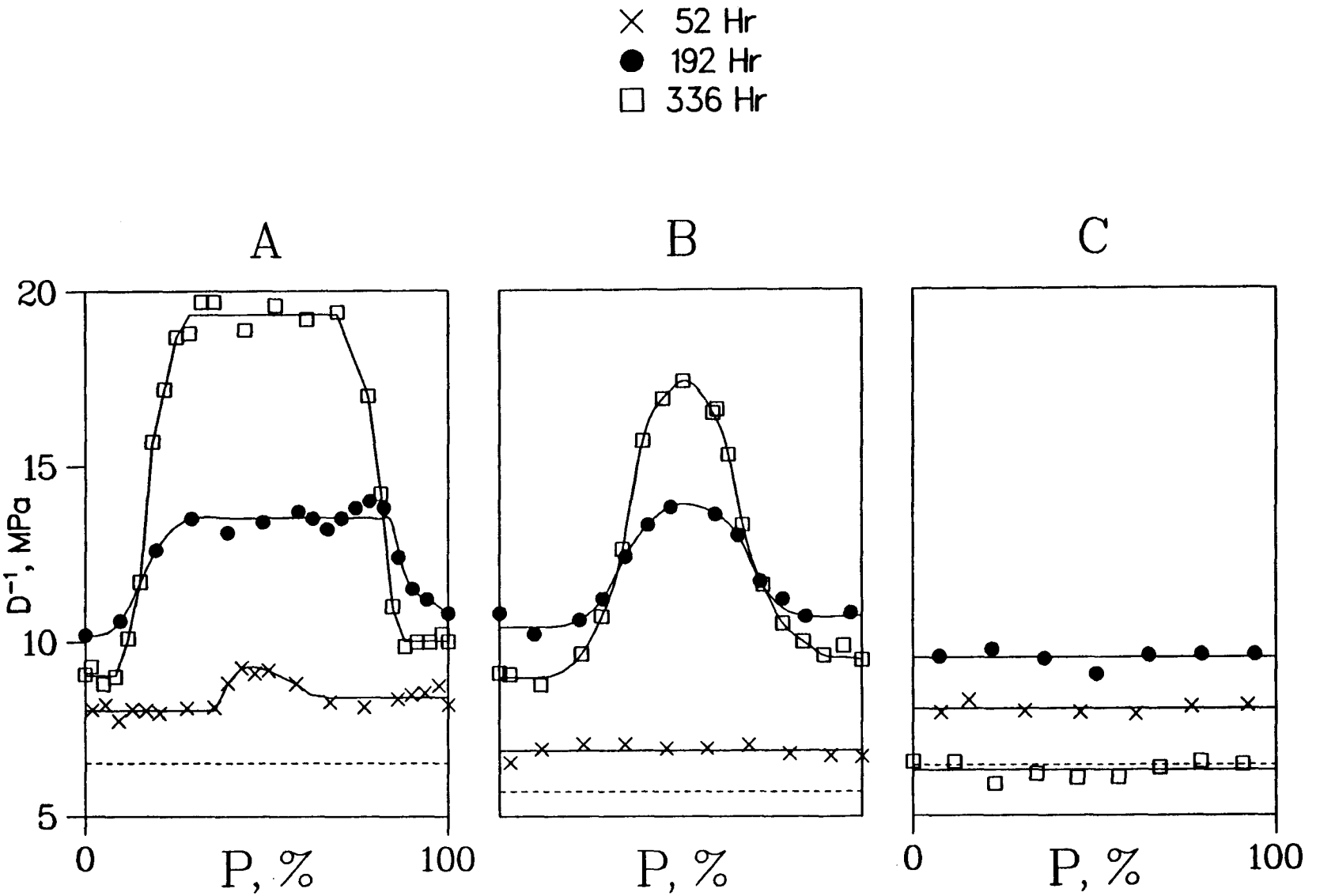

2.7 mm (A), 1.7 mm (B) AND 0.7 mm (C) THICK EPR AFTER GAMMA AGING

EPR–IRRADIATED

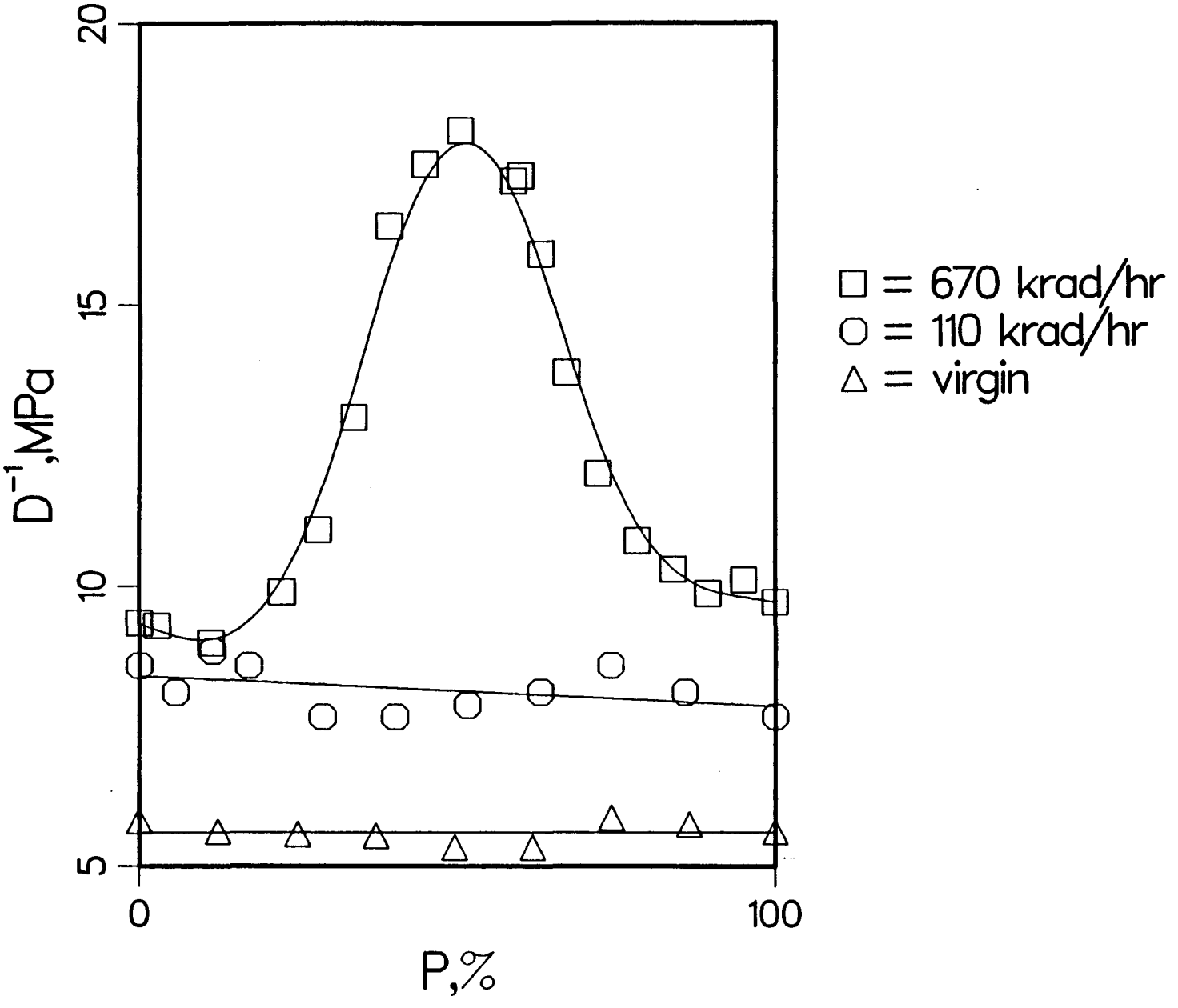

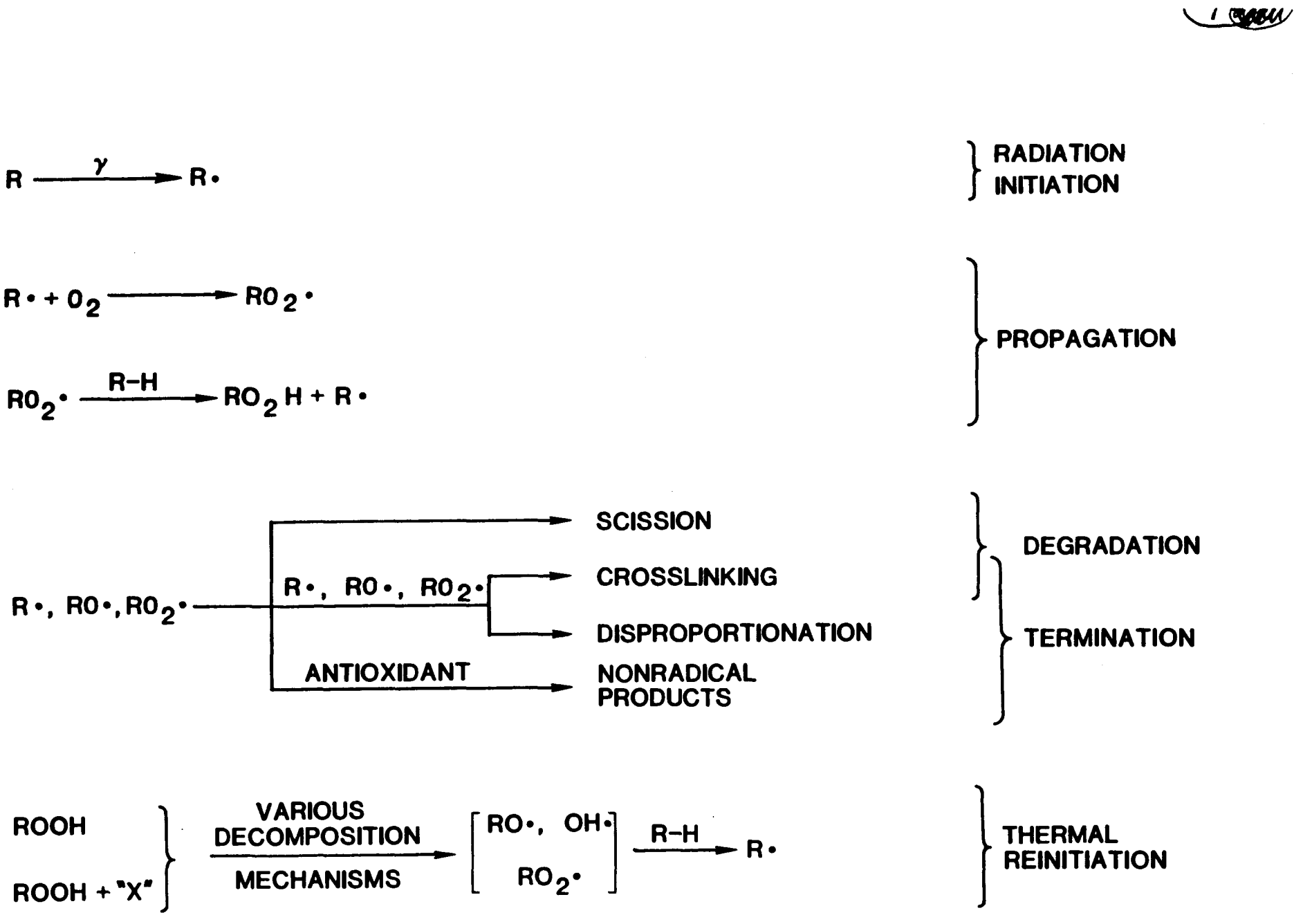
R → R•
γ
RADIATION INITIATION
R• + O2 → RO2•
RO2• + R-H → RO2H + R•
PROPAGATION
R•, RO•, RO2•
R•, RO•, RO2•
SCISSION
CROSSLINKING
DISPROPORTIONATION
ANTIOXIDANT
NONRADICAL PRODUCTS
DEGRADATION
TERMINATION
ROOH
ROOH + "X"
VARIOUS DECOMPOSITION MECHANISMS
RO•, OH•
RO2•
R-H
R•
THERMAL REINITIATION

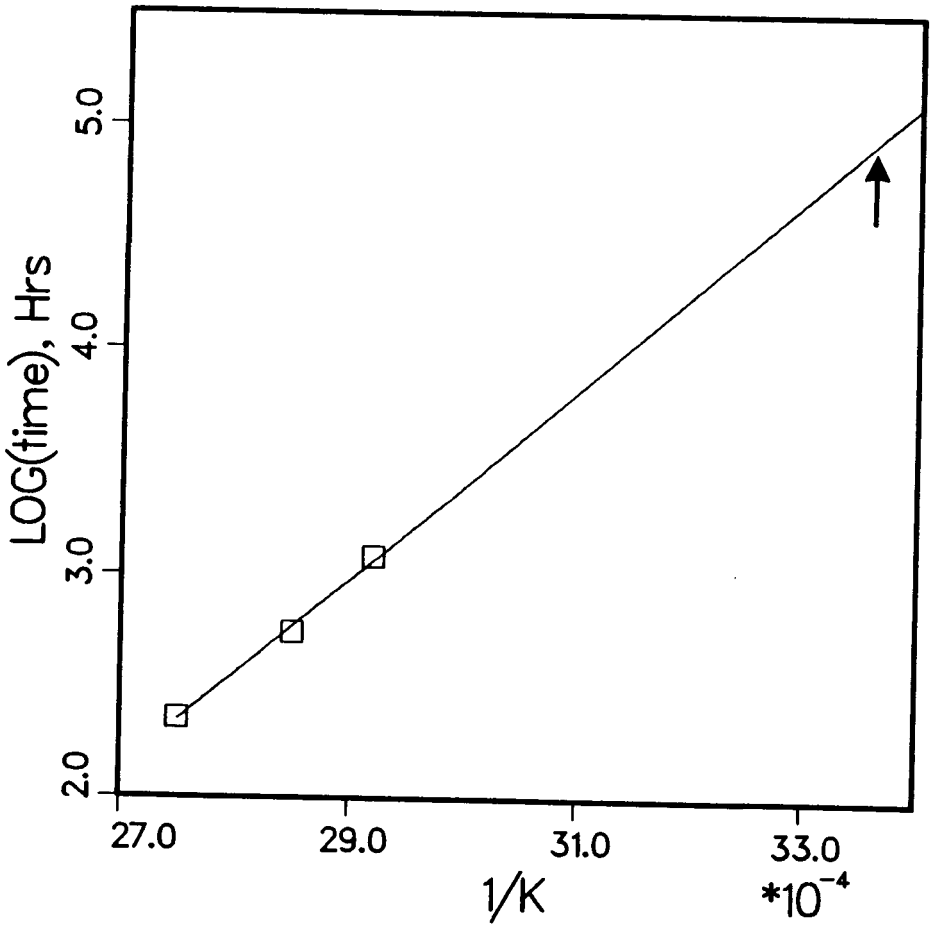
LOG(time), Hrs
5.0
4.0
3.0
2.0
27.0
29.0
31.0
33.0
1/K
*10⁻⁴

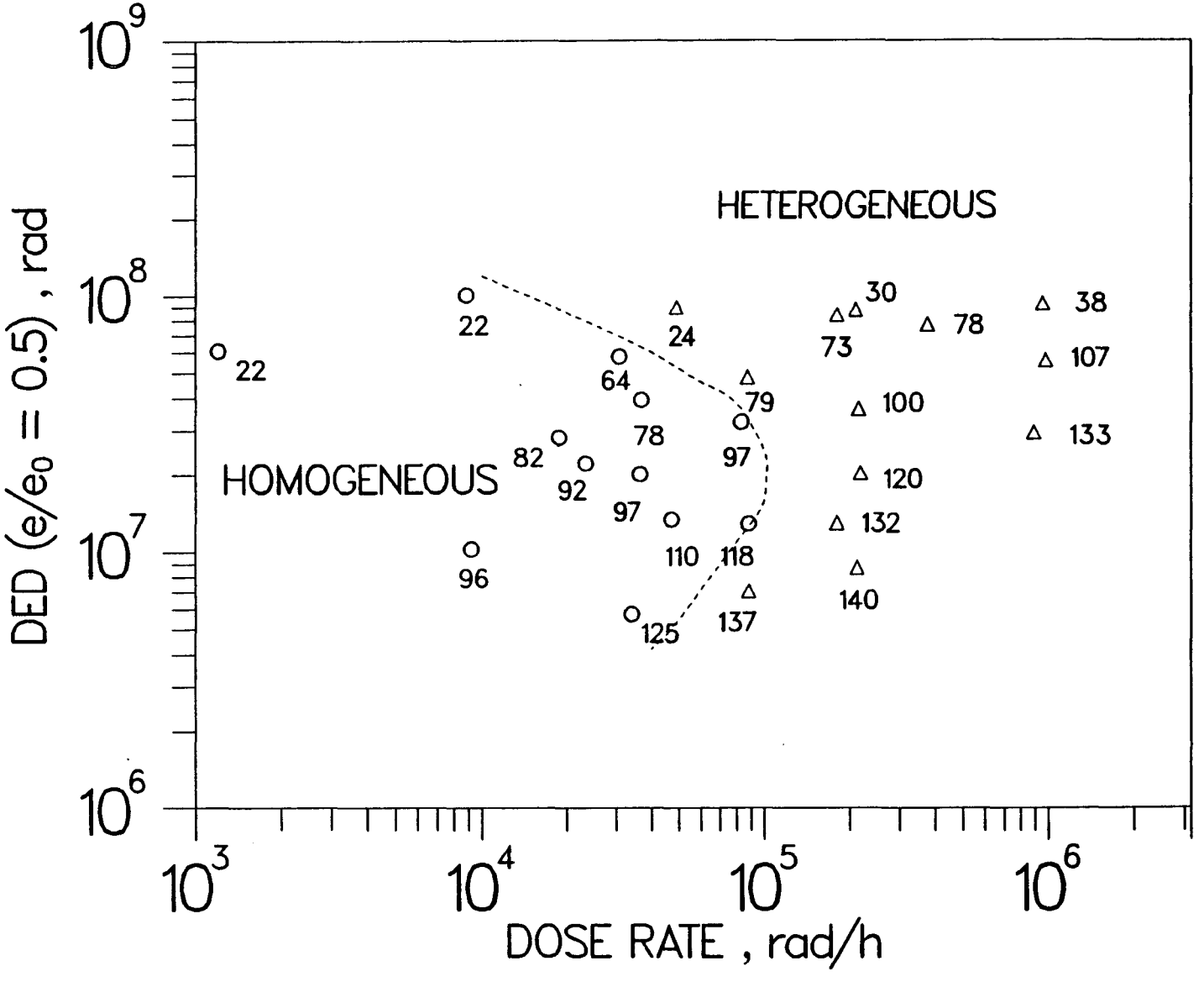
HETEROGENEOUS
HOMOGENEOUS
DED (e/e0 = 0.5) , rad
DOSE RATE , rad/h
10^9
10^8
10^7
10^6
10^3
10^4
10^5
10^6
22
22
24
64
79
78
97
82
92
97
110
118
96
125
137
30
73
78
38
107
100
133
120
132
140

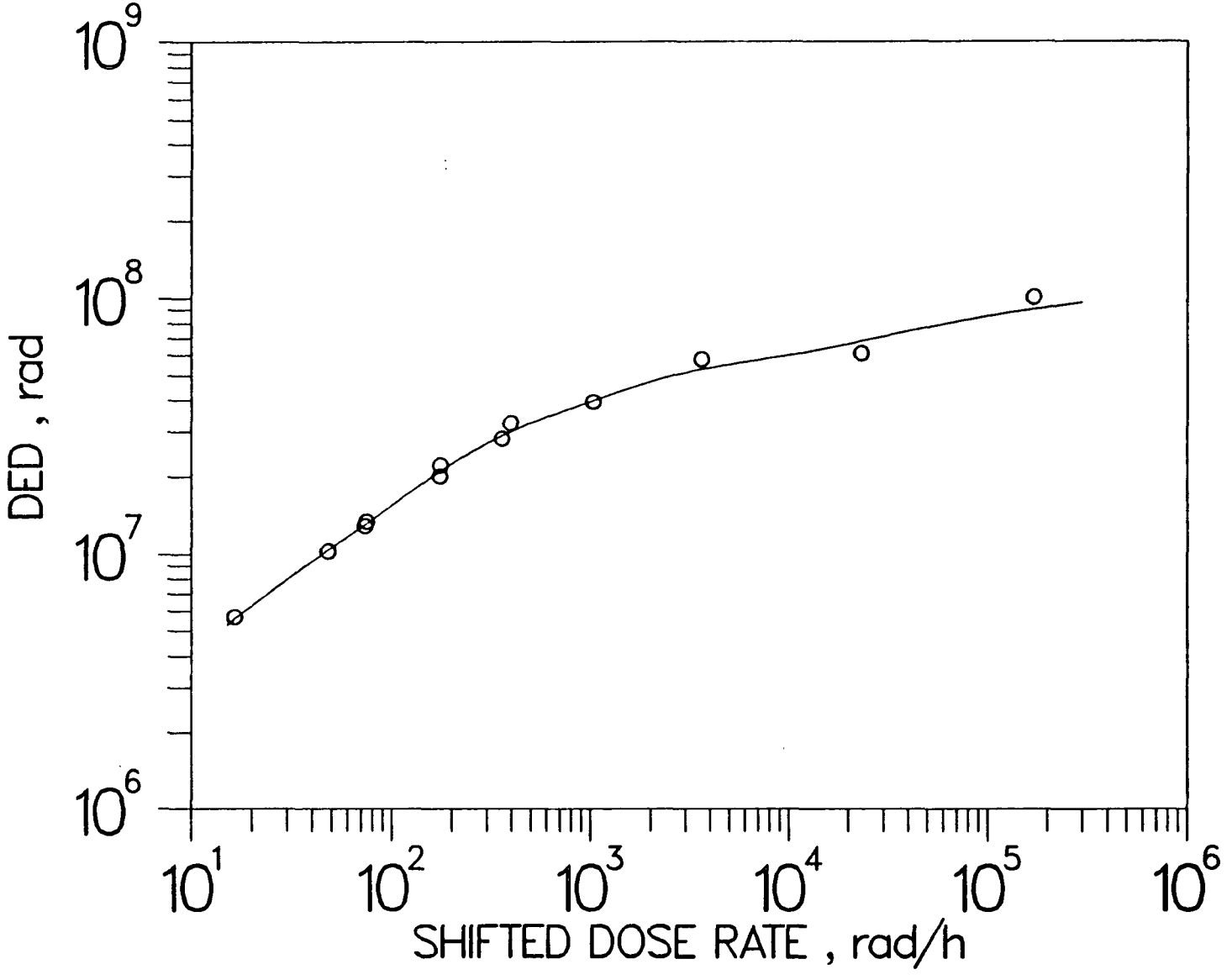
10^9
10^8
10^7
10^6
DED , rad
10^1
10^2
10^3
10^4
10^5
10^6
SHIFTED DOSE RATE , rad/h

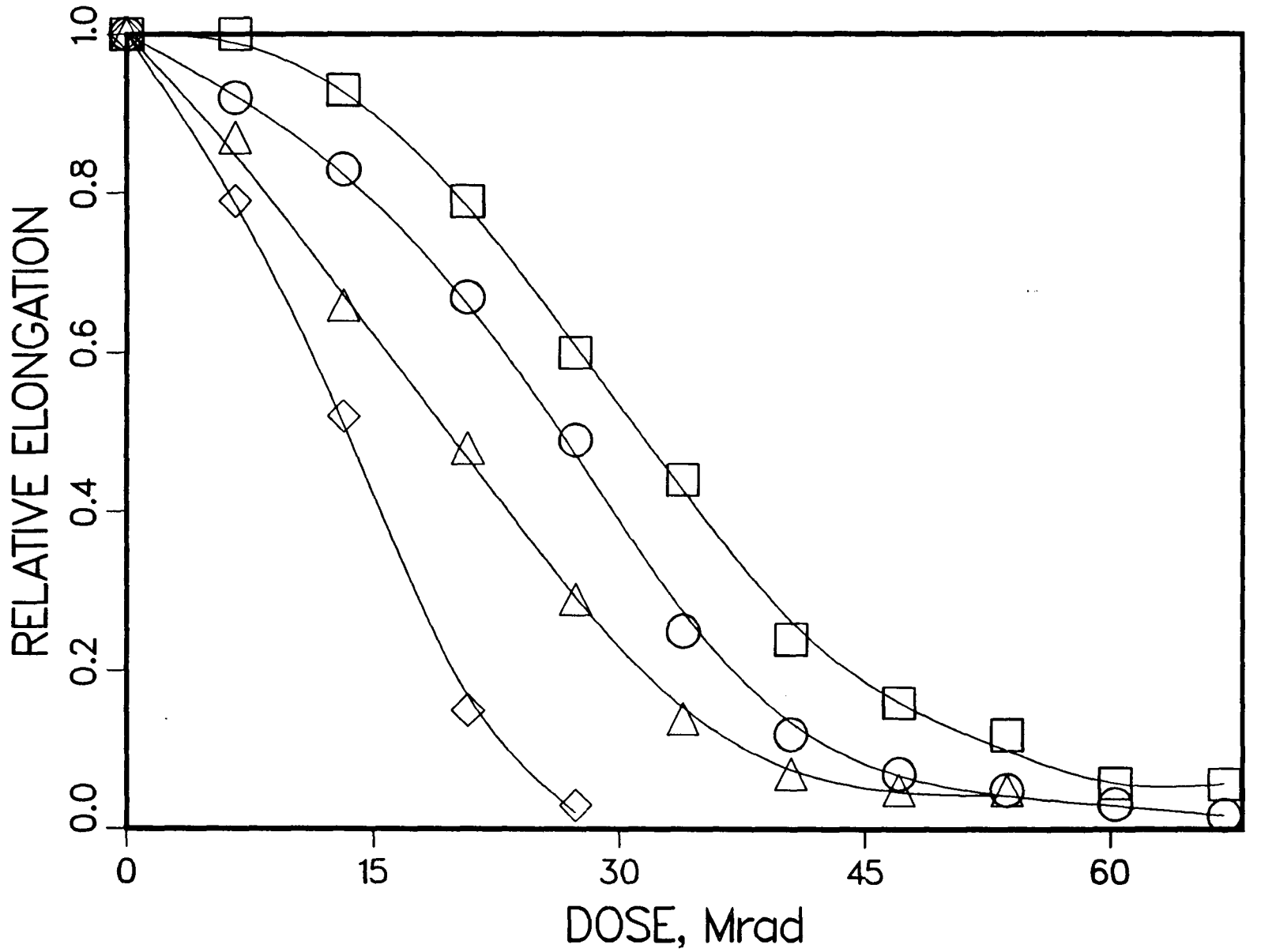
RELATIVE ELONGATION
1.0
0.8
0.6
0.4
0.2
0.0
0
15
30
45
60
DOSE, Mrad

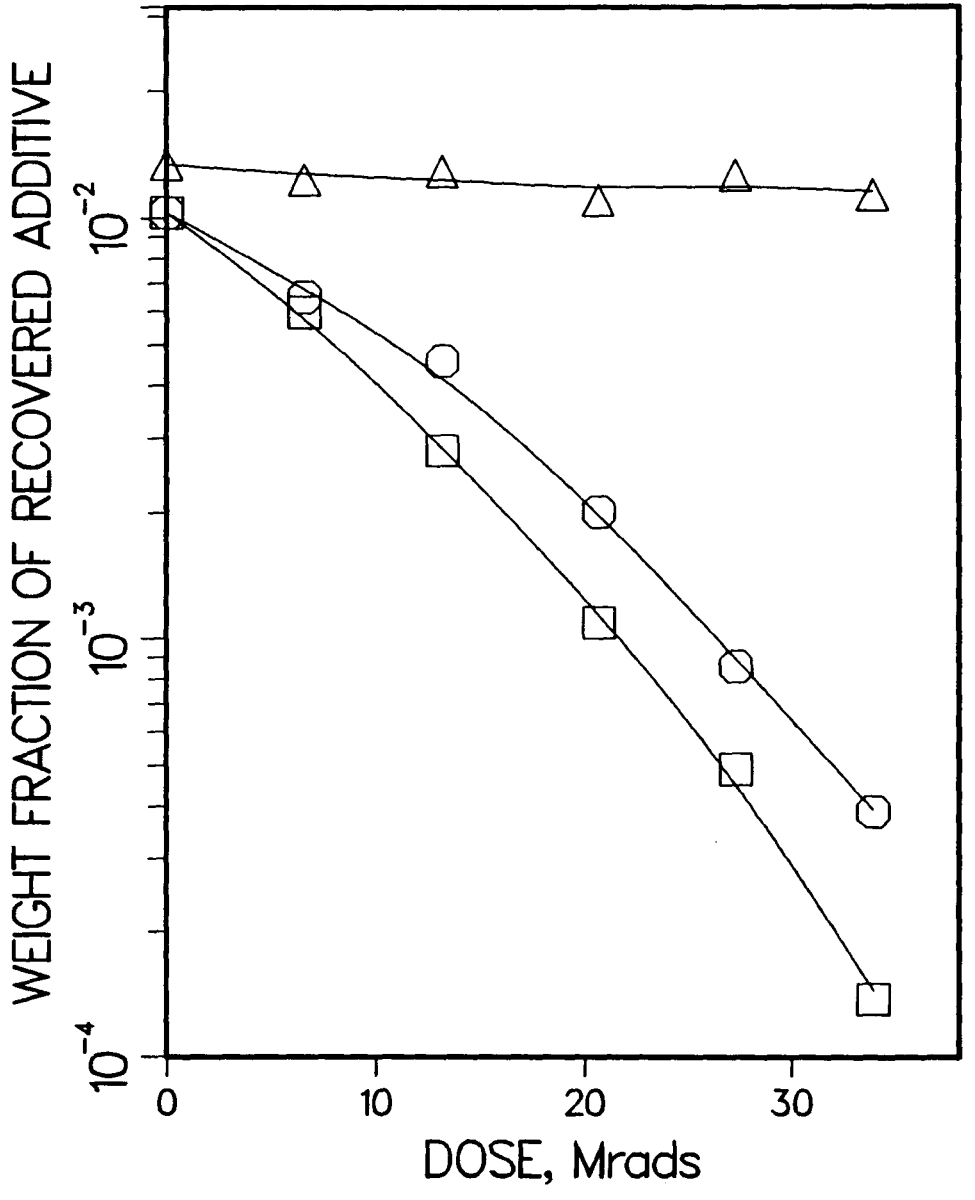
WEIGHT FRACTION OF RECOVERED ADDITIVE
10^{-2}
10^{-3}
10^{-4}
0
10
20
30
DOSE, Mrads

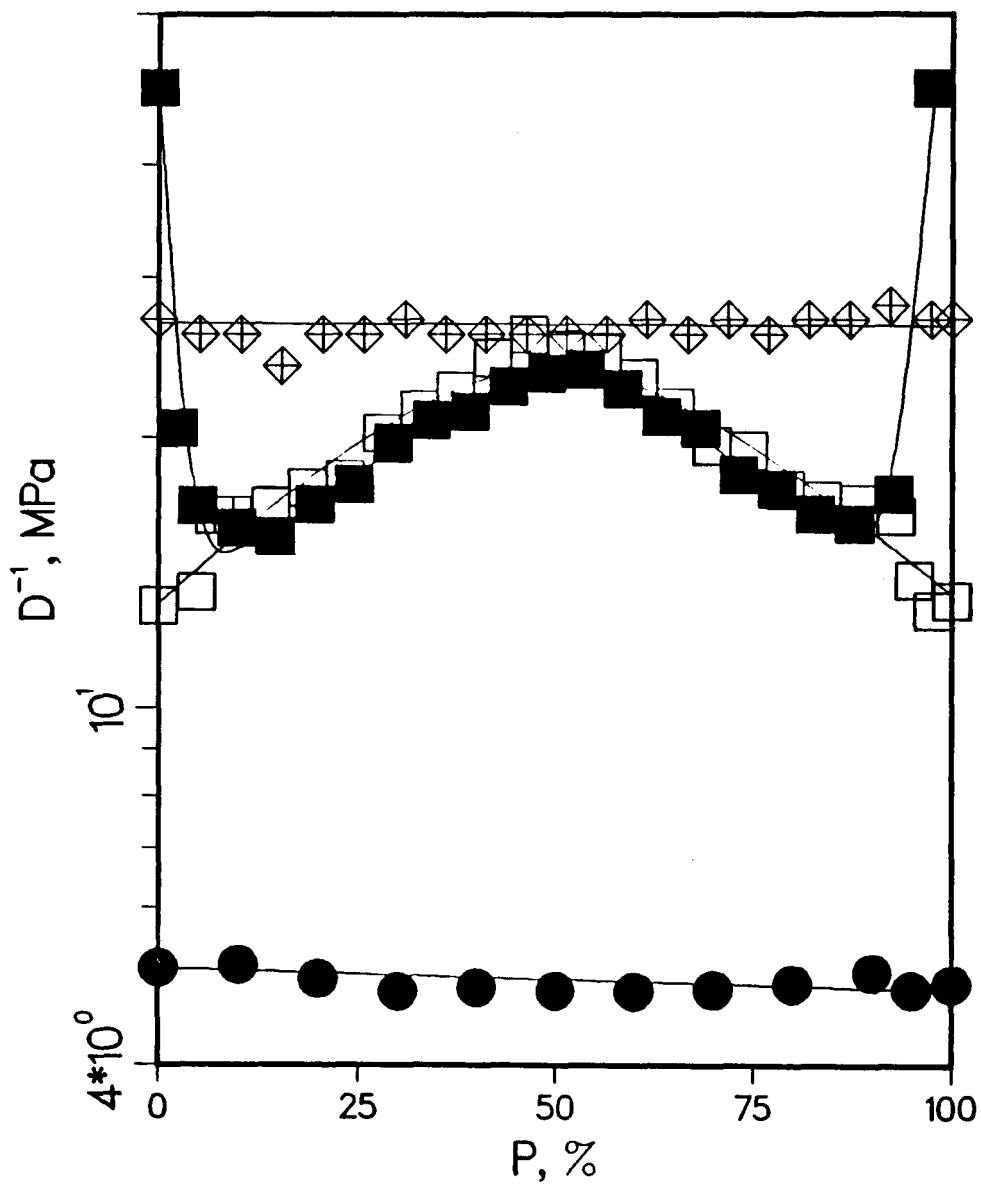
D⁻¹, MPa
10¹
4*10⁰
0
25
50
75
100
P, %